ANALYSES AND COMPARISON OF MUDBRICK BUILDING MATERIALS FROM SEYİTÖMER HÖYÜK EARLY BRONZE AGE-III AND MIDDLE BRONZE AGE

SEYİTÖMER HÖYÜK ERKEN TUNÇ ÇAĞI-III VE ORTA TUNÇ ÇAĞI KERPIÇ YAPI MALZEMELERININ ANALIZLERI VE KARŞILAŞTIRMASI

Makale Bilgisi | **Article Info**

Başvuru: 10 Ekim 2023 | Received: October 10, 2023
Hakem Değerlendirmesi: 3 Kasım 2023 | Peer Review: November 3, 2023
Kabul: 6 Haziran 2024 | Accepted: June 6, 2024

DOI: 10.22520/tubaar.1374064

Eda TAŞÇI* - Hale YILDIZAY - Nazan ÜNAN*** - Merve Dağcı TEKİN******

ABSTRACT

Archaeological excavations have been carried out intermittently since 1989 in Seyitömer Höyük, a medium-sized mound located 25 km northwest of Kutahya. Seyitömer Höyük excavation, a salvage excavation, aims to excavate the entire pile. The layers unearthed during the excavations are essential in that they are as a whole and reveal the architectural plans. The Middle Bronze (MBA) and Early Bronze III (EBA-III) periods and layers were unearthed during the rescue excavation in 2021 at the mound. In this study, the mudbrick samples recovered from the settlements and buildings of the MBA and EBA-III layers of Höyük were defined and named. 10 mudbrick samples taken from specific periods and locations were determined, and their periodical properties were determined. Chemical compositions of mud brick samples were analyzed by X-ray fluorescence (XRF), and mineralogical, compositions were determined by X-ray diffraction (XRD). The bond structure of the mudbrick samples was confirmed by comparing them with the Fourier transform infrared spectroscopy (FTIR) analysis results. In addition, some of the mudbrick, which are thought to have been exposed to periodic fires, were selected, and subjected to scanning electron microscopy (SEM) analysis and energy dispersive X-ray (EDX) analysis.

Keywords: Mudbrick Building Materials, Seyitömer Höyük, Early Bronze Age-III, Middle Bronze Age

* Prof. Dr., Kütahya Dumlupınar Üniversitesi, Fakülte, Bölüm,
e-posta: eda.tasci@dpu.edu.tr, ORCID: 0000-0003-3346-8833
** Dr. Öğr. Üyesi, Kütahya Dumlupınar Üniversitesi, Fakülte, Bölüm,
e-posta: hale.yildizay@dpu.edu.tr, ORCID: 0000-0002-3896-9912
*** Öğr. Gör., Kütahya Dumlupınar Üniversitesi, Fakülte, Bölüm,
e-posta: nazan.unan@dpu.edu.tr, ORCID: 0000-0001-6517-9441
**** Dr. Öğr. Gör., Kütahya Dumlupınar Üniversitesi, Fakülte, Bölüm,
e-posta: merve.dagci@dpu.edu.tr, ORCID: 0000-0001-6639-8080

ÖZET

Kütahya ilinin 25 km kuzeybatısında yer alan orta ölçekli bir höyük olan Seyitömer Höyük'te 1989 yılından beri aralıklarla arkeolojik kazılar gerçekleştirilmektedir. Kurtarma kazısı niteliği taşımakta olan Seyitömer Höyük kazısında höyüğün tamamının kazılması hedeflenmektedir. Yapılan kazılarda açılan tabakalar, bütün halinde ve mimari planları da ortaya çıkaran şekilde olması açısından önem taşımaktadır. Höyük'te gerçekleştirilen kurtarma kazısında Orta Tunç (MBA) ve Erken Tunç III (EBA III) dönemleri ve tabakaları ortaya çıkarılmıştır. Bu çalışmada özellikle MBA ve EBA III tabakalarının yerleşim yeri ve mekânları içinden ele geçirilen yapılardaki kerpiç bünyeleri tanımlanarak adlandırılmıştır. Ele geçen dönemleri ve konumları belli mekanlardan alınan 10 adet kerpiç örneği karakterize edilerek dönemsel özellikleri analiz edilmiştir. Kerpiç numunelerine ait kimyasal kompozisyonlar X-ışını floresansı (XRF), mineralojik ve faz kompozisyonları X-ışını difraksiyonu (XRD) ile belirlenmiştir. Kerpiç örneklerinin yapısında bulunan bağ yapı özellikleri Fourier dönüşümlü kızılötesi spektroskopi (FTIR) analiz sonuçları ile kıyaslanarak teyit edilmiştir. Ayrıca dönemsel yangınlara maruz kalmış olduğu düşünülen kerpiç örneklerinin bazıları seçilerek SEM analizi ve EDX analizine tabi tutularak kerpiçlerde oluşan bozunma miktarındaki farklılıklar, dönemsel olarak kullanılan killerdeki yapısal farklılıklar ortaya konulmuştur.

Anahtar Kelimeler: Seyitömer Höyük, Erken Tunççağı, Ortatunççağı, Kepiç Malzemeler

INTRODUCTION

Seyitömer Höyük is located within the lignite reserve area of Çelikler Seyitömer Electricity Generation Company, located near the town of Seyitömer, 25 km northwest of Kutahya city center (Fig. 1). While the Seyitömer Höyük excavation area, located within the Seyitömer Lignite Basin, had a high hill topography before the excavations started, the hill topography reached a lower point in November 2021. The last aerial photograph formed as of the end of the 2021 excavation period is given (Fig. 2).

Seyitömer region, which has a continental climate, is geologically composed of river and lake sediments. According to Ozcan (1986), the Seyitömer formation is Miocene in age. It consists of five members: the sandstone-pebblestone member, the mudstone-claystone member, the laminated shale member, the siliceous limestone member, and the clay-limestone member.

In the south and west of the Seyitömer Lignite basin, the suffice-level clay-limestone consists of grayish-white clayey limestone and whitish-gray-colored intermediate levels (Yanık, 1997). The fact that this region, whose geological features were detailed, is a clay basin that has many benefits for human beings has a significant effect on selecting this region as a settlement within the archaeological chronology. Excavations in Seyitömer Höyük, initiated by the Eskisehir Museum Directorate in 1989 (Aydın *et al.,* 1991), were continued by the Afyon Museum Directorate between 1990-1995 (Topbas, 1992; Topbas, 1993; Topbas, 1994; Ilaslı, 1996), and the Kutahya Dumlupınar University Archaeology Department carried out studies between 2006 and 2014 (Bilgen *et al.,* 2015). The excavations started in 2019 under the presidency of the Kutahya Museum Directorate are continuing. Based on the studies, the stratification is in the form of I- Roman Period, II- Hellenistic Period, III- Achaemenid (Iron Age), IV- Middle Bronze Age (MBA), V- Early Bronze Age III (EBA-III), VI- Early Bronze Age IIIA (Unan *et al.,* 2020).

The VI. layer is the transition layer dated between EBA-III and EBA-II, and the plan features of the EBA-III settlement in terms of architecture started to become evident in this layer VI a was dated to EBA II and a part of this layer was exposed, and it was determined that the settlement was built in accordance with the Anatolian settlement plan. There are bull-headed hearths, domed ovens, and storage compartments in the spaces created alongside common walls (Unan *et al.,* 2021). The level dated to EBA III has four phases and shows a regular settlement plan.

Figure 1. Map showing the location of Seyitomer Hoyuk/ *Seyitömer Höyüğün konumunu gösteren harita.*

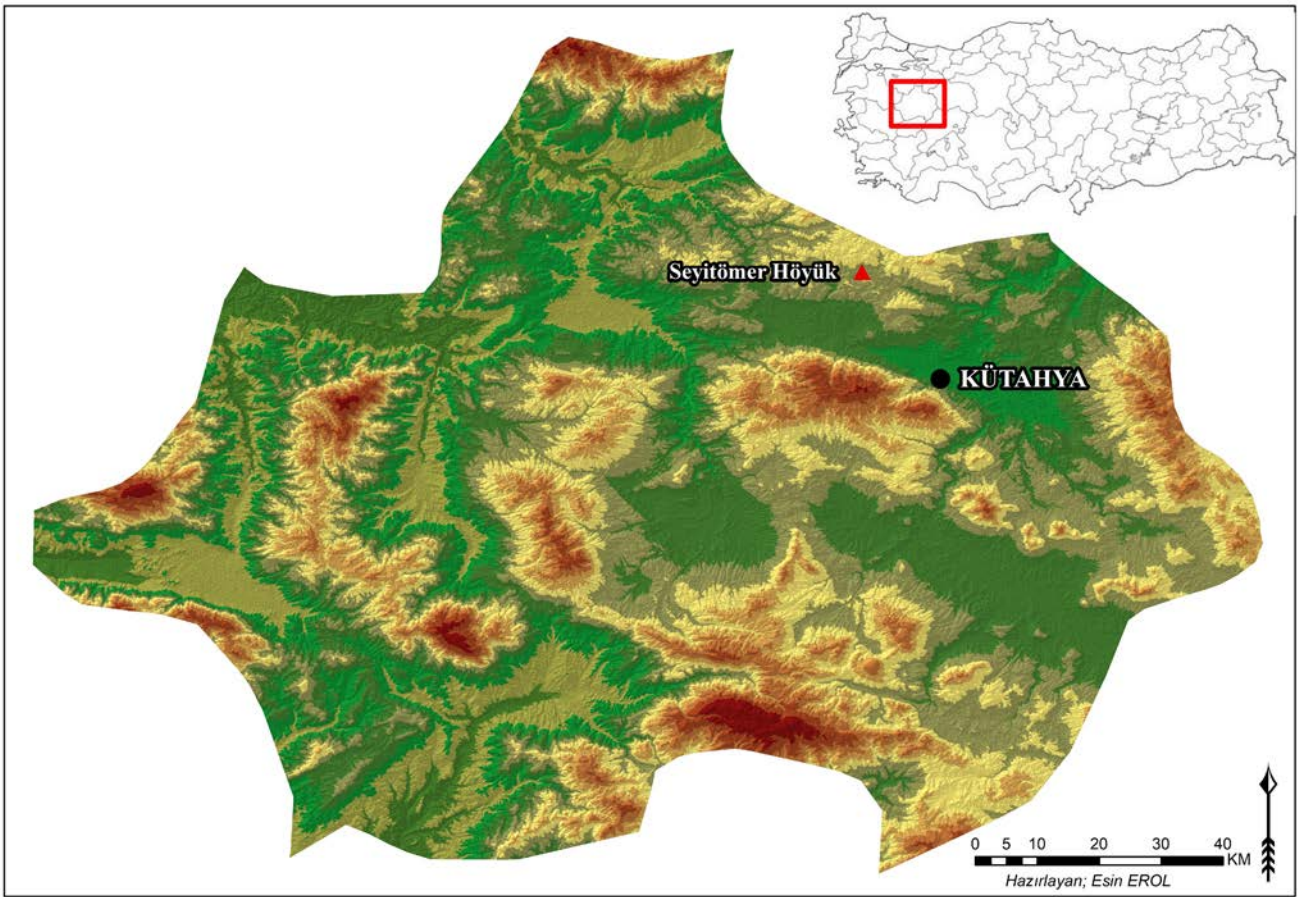

DOI: 10.22520/tubaar.1374064

Figure 2. Aerial photograph of Seyitomer Hoyuk in 2021/ *Seyitömer Höyük 2021 yılı hava fotoğrafı.*

The settlements surrounded by walls contain workshop spaces, religious structures, and administrator buildings. There are bull-headed hearths, dome ovens, and partitions among the interior equipment of the areas (Unan *et al.,* 2020). Figure 3 shows the plan of the A, B, C, and D phases of the Level V of Seyitömer Höyük. The use of mud brick in EBA-III (Level V) settlement appears similarly in every step. In addition, in Figure 4, the intermediate mudbrick wall of Seyitömer Höyük V/D phase space 82 is seen. As seen in the photo, the intermediate wall can be used as a common wall in more than one space. The double-faced, solidly built walls are often raised with stone up to the roof.

Figure 3. Plan of the levels A, B, C and D of Seyitomer Hoyuk level V / *Seyitömer Höyük V. tabaka A, B, C ve D evrelerinin planı*

Figure 4. Seyitomer Hoyuk Phase V/D, Room 82, mud brick partition / *Seyitömer Höyük V/D evresi 82 no'lu mekan, kerpiç ara duvar.*

In phase D, one wall of the space was made of mudbrick or was used to divide a large room into two. Fig. 5 shows the mudbrick detail of Seyitömer Höyük Phase V/D (Unan, 2019). In addition, mud brick was used to create storage compartments, usually located in the corners of the spaces. In phase C, although the use of stone in the construction of the walls continues, one of the room's walls was built with mud brick, or the wall built with stone was raised with mudbrick. The average dimensions of the mudbricks used in this phase range from 0.01 x 0.35 x 0.35 m to 0.10 x 0.40 x 0.70 m (Unan, 2013). In this phase, the use of mudbrick is more intense than in other phases (Bilgen *et al.,* 2015). In Phase B, two rooms were built with mudbrick on a stone foundation and only mudbrick was used to divide the rooms. In phase A, mud-brick piles were encountered in a few rooms.

Figure 5. Seyitomer Hoyuk V/D phase mudbrick detail / *Seyitömer Höyük V/D evresi kerpiç detay.*

DOI: 10.22520/tubaar.1374064

Based on these data, it is possible to say that the walls of some rooms were raised with mudbrick. The mudbrick dimensions used in this phase range from 0.30 x 0.50 x 0.65 m to 0.10 x 0.20 x 0.40 m (Bilgen, 2012).

Level IV, dated as MBA, has three phases and is surrounded by a robust fortification system. The buildings were built by bricklaying, and structures with one to three rooms were identified. Inside the spaces are horseshoe hearths, ovens, compartments, and benches, while outside are circular silos (Unan, 2019). When the Middle Bronze Age layer is evaluated architecturally, it can be said that the materials used in architecture consist of rubble stone, clay soil, and wood. Space floors are usually compacted soil floors. In some examples, it is seen that some rooms or sections of the building are stone pavement, while other parts are built on an earthen base (Bilgen and Bilgen, 2015). It was found in the MBA layer, especially in phases B and C, in the form of mud bricks found in piles on the stone walls and inside the rooms (Yuzbasıoğlu, 2010). The walls were generally raised with stones up to the roof. In some examples, it was found that stone was introduced to a certain height, and the remaining upper part was raised with mudbrick blocks. Although the dimensions of the mud brick bricks vary, they appear to be 0.10 x 0.45 x 0.50 m on average (Unan, 2013).

Clay, the primary raw material of mud brick-based building materials, is a naturally occurring material that mainly consists of fine-grained minerals, becomes plastic when sufficient water is added and can harden by drying and firing. The definition of "clay mineral" is used for layered silicate group minerals and minerals that give plasticity to clays and harden by drying and firing (Bilgen and Olgun, 2012).

It is known that clay, used as a building material since the Neolithic Period, was used in different ways. Mud brick is a building material obtained by mixing straw or other vegetable fibers (such as reed-like plants, straw, and tree branches) into clayey soil, kneading, then pouring into molds and drying in the open air. Suitable soil, additives, and soil-water mixture are essential to preparing mud brick mud. The shrinkage that occurs after drying affects the self-supporting strength of the structure (Ozdoğan, 1996).

The mud brick-based building material, the production stage of which is elementary, is obtained by mixing gravel, straw, and sometimes animal hair with clay soil and water, then pouring it into molds and drying it in the sun (Akkas, 2011). The clay in the soil acts as a binder in the mud brick mixture, while the gravel, straw, and water mix provide plasticity to the ground so that the earth can be molded. The energy required for drying and gaining strength is supplied by the sun. Since 9000 BC, mudbrick has been widely used as the material for different structures such as houses, barns, pens, and poultry (Dirican and Akyol, 2019).

The mudbricks, which are also the subject of this article, are used periodically in almost every layer. The study aims to analyse a total of about 750 years of mudbrick samples from the four phases of the EBA III period to the following MBA period. As a result we can say that EBA and MBA are different periods. Th that similar substances were added to the mudbrick when it was made. In addition, as a result of exposure to a certain temperature in the settlement, all to compare the heat exposure rates of the mudbrick samples recovered is also among the aims of the article.

MATERIAL AND METHODS

A general aerial photograph of the EBA-III periods D and the V/D phase of the MBA period from the Seyitömer Höyük region in 2021 from the top view is given in Fig.1. In Fig.2, the photographs of the places where the mudbrick structures belonging to the EBA-III period and the MBA period were found during the V/D phase excavation process can be seen.

One-to-one scale photographs of the representative samples belonging to the EBA-III period and the MBA period are given in Fig.4 and Fig.5, respectively. In Table 1, the archaeological period of the mudbrick samples (as Early Bronze and Middle Bronze), the year and place, the archaeological code, and the type (in which part of the finds settlement was taken and prepared for analysis) are defined.

After completing the definition of the archaeological site and finds, the stages of preparation of the finds for archaeometric analysis were started.

Table 1. Naming the EBA III and MBA mud brick samples / *EBA III ve MBA kerpiç buluntularının adlandırılması.*

Code	Artefacts Archaeological Period	Find Year, Context and Archaeological Code
EBA-III-1	EBA-II-III VI (Transition)	Place 6 B
EBA-III-2	EBA-III V/D	Place 67 D
EBA-III-3	EBA-III V/D	Place 51 A
EBA-III-4	EBA-III (V/D)	Place 51
EBA-III-5	EBA-III V/C	Place 72
EBA-III-6	EBA-III V/C	F-13 Place GD Corner
EBA-III-7	EBA-III (V/B)	Place 10
MBA-1	MBA (IV/C)	Place 1
MBA-2	MBA (IV/C)	K-7 Place 1
MBA-3	MBA (IV)	L-15 Place 4

In this research paper, a characterisation study was carried out on the clay samples obtained from the region and mud brick samples obtained from the excavations, which are thought to have been seen in the fire.

Each supplied mud brick sample was subjected to grinding and sieving processes below 63 µm. To determine the quantitative ratio of the oxides in the internal structure of the powdered samples and to examine their standard properties in detail, a chemical analysis of the samples was made with X-ray fluorescence (XRF) (Spectro X-Lab 2000). The chemical analysis results of 12 samples are given in Table 2.

This analysis was performed using the ATR (Attenuated total reflectance) method, in which direct analyses of powder samples can be carried out in the Bruker brand Alpha-model FTIR device, with a resolution of 4 cm^{-1} in the wavelength range of 400-4000 cm^{-1}, and the average of the measurement result and spectra were obtained.

By the chronological order of the findings, the microstructural and microchemical properties of the selected samples were examined by the SEM-EDX technique, considering the fire exposure rates. Scanning electron microscopy is an analysis technique in which electrons are used instead of light as a source and scans

Table 2. Chemical analysis results of EBA III and MBA mud brick samples / *EBA III ve MBA kerpiç buluntularının kimyasal analiz sonuçları.*

CODE	SiO_2	Al_2O_3	Na_2O	CaO	K_2O	MgO	TiO_2	Fe_2O_3	Cl	P_2O_5	SO_3	MnO	LOI
EBA III-1	53.5	11.0	0.6	7.6	2.5	4.4	0.4	6.5	0.1	0.3	0.1	0.2	12.5
EBA III-2	36.8	7.9	0.3	19.2	2.4	5.5	0.3	3.9	0.1	0.3	0.4	0.1	22.1
EBA III-3	48.7	9.8	0.4	15.2	2.2	5.8	-	5.4	0.09	0.5	0.08	0.2	10.8
EBA III-4	39.2	8.5	0.3	21.8	1.8	5.5	0.3	4.5	0.1	0.5	0.1	0.1	16.7
EBA III-5	58.8	12.5	0.6	7.8	3.1	3.5	0.5	6.3	0.1	1.1	0.2	0.2	4.9
EBA III-6	57.9	14.0	1.2	7.9	2.5	4.3	0.5	5.3	-	0.4	0.1	0.1	5.2
EBA III-7	60.9	14.0	0.9	2.7	2.6	2.3	0.6	9.2	0.1	0.2	0.1	0.2	5.6
MBA-1	46.9	10.1	0.6	12.9	2.8	4.8	0.4	4.9	0.1	0.3	0.1	0.1	15.5
MBA-2	35.7	7.1	0.3	16.8	1.7	9.1	0.2	3.9	-	0.3	0.1	0.1	24.2
MBA-3	67.0	12.4	0.8	4.5	2.4	2.2	0.5	5.8	-	0.4	0.1	0.1	3.5
Clay	37.2	7.7	0.5	11.5	1.06	7.2	0.2	3.6	-	0.2	0.2	0.1	30.0
Fired clay	53.3	9.9	0.3	17.4	1.6	8.9	0.3	6.2	0.1	0.4	1.1	0.2	-

LOI: Loss on inginition

In order to determine the mineralogical properties of the mudbrick samples used as architectural structures in this period, mineralogical analyses were performed by XRD method and the changes that occurred in mudbrick structures over time were defined. X-ray diffraction (XRD) analyses (Rigaku Miniflex X-ray diffusion) were performed on samples ground into fine powder in an agate mortar. In the analysis of the samples, Cu Kα radiation, 20 mA, 40 kV, speed 0.5°/min was used. Measurements were made with a 2θ angle in the range of 5°-70°, with a step size of 0.02°.

In the study, FTIR analysis, which is the most preferred one in the characterization of natural organic materials, especially organic compounds of ancient building materials, was used. Fourier transform infrared spectroscopy (FTIR) method can simultaneously collect high spectral resolution data over a wide wavelength range.

the sample's surface to be analyzed as high-energy strips. Microstructural/microchemical properties of materials are determined by SEM/EDX analysis. For this purpose, the FEI NovananoSEM 650 model SEM/EDX device was used in this study. Before the analysis, the mud brick finds were coated with platinum in the coating device and made conductive. The chemical compositions of the samples were determined by EDX spectra taken at different scales. EDX results are considered as elements and oxide forms.

RESULT AND DISCUSSION

In this study, a chronological classification of 12 mudbrick building material finds belonging to the EBA III period and the V/D phase of the MBA period recovered from the Seyitömer mound, located 25 km northwest of Kütahya province, during the excavations of 2021.

DOI: 10.22520/tubaar.1374064

The fire processes and burning rates that the mudbrick material finds are thought to have been exposed to according to their periods were evaluated through characterization studies. In addition, the clay obtained from the region was analyzed and compared with the analysis of EBA III and MBA mudbrick finds.

In chemical analyses, the percentages of oxides such as SiO_2, Al_2O_3, CaO, MgO, K_2O, Na_2O, and Fe_2O_3 in the samples are generally determined. The mineral type (e.g. for clays) can be determined by comparing the percentages determined by analysis with the oxide results obtained from the sample. For example, SiO_2/Al_2O_3=1.3 in pure kaolinite (Qiu *et al.,* 2004). Values greater than this indicates the presence of clay and free quartz in the structure. High fire loss also indicates that the sample contains volatile substances such as CO_3 and SO_4. Alkaline earth and oxides greater than 1% indicate the presence of mica, feldspar, and alkalis in the structure. Table 2 shows the chemical analysis results of the Early Bronze III and Middle Bronze Age samples. When evaluating the results of the chemical analysis, it can be said that the clay soil obtained from the region contains a high percentage of CaO (11.52%). In addition, the clay soil has a SiO_2/Al_2O_3 ratio of 4.83 and contains free quartz. After firing, the SiO_2/Al_2O_3 ratio of the clay soil increased to 5.34. In addition, the fire loss in the clay soil after firing is zero.

In Table 2, CaO/SiO_2, Fe_2O_3/SiO_2, and fire loss ratios of EBA III specimens and MBA specimens were shown on the graph to show the properties of adobe building materials defined by chemical analysis in terms of their fire exposure (proportionally) and the specimens that were thought to be most exposed to fire were shown on the graph comparatively (Fig. 6). Fig. 6, according to the comparison graph of the fire loss, CaO/SiO_2, Fe_2O_3/SiO_2 ratios of the EBA III samples, the EBA III-7 sample is the most exposed to fire. It is followed by EBA III-6, EBA III-5 and EBA III-1. EBA III-2, EBA III-3, and EBA III-4 represent the less fire-exposed group samples.

Figure 6. Comparison of loss on ignition, CaO/SiO_2 and Fe_2O_3/SiO_2 ratios of EBA-III mud brick samples / *EBA III kerpiç buluntularının ateş zaiyatı, CaO/SiO2 ve Fe2O3/SiO2 oranlarının karşılaştırması.*

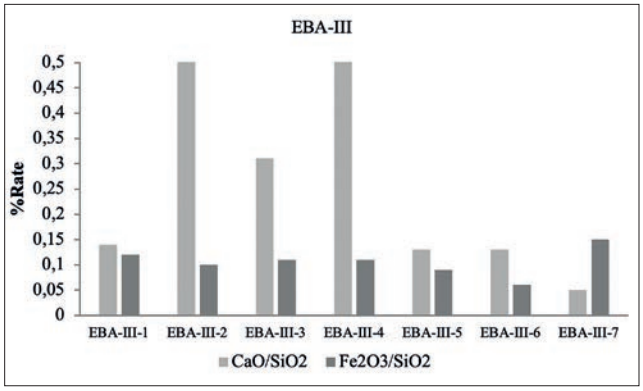

Fig. 7, the proportional comparison graph of fire loss, CaO/SiO_2, and Fe_2O_3/SiO_2 of the Middle Bronze samples shows that MBA-2, MBA-1, and MBA-3 are the most fire-exposed finds, respectively.

Figure 7. Comparison of loss on ignition, CaO/SiO_2 and Fe_2O_3/SiO_2 ratios of MBA mud brick samples. loss on ignition / *MBA kerpiç buluntularının ateş zaiyatı, CaO/SiO2 ve Fe2O3/SiO2 oranlarının karşılaştırması.*

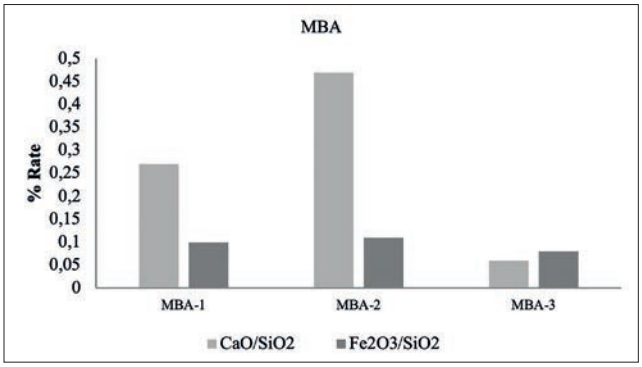

When the XRD analysis of the clay obtained from the Seyitömer region and the same clay after firing 1000 ℃ is analyzed, it is seen that the clay obtained from the region is mainly composed of quartz, anorthite, and muscovite phases. The amorphous ratio of the raw clay is higher before firing, while the crystallization rate increases after firing. It can be said that thanks to the low Al2O3 ratio in the clay, the melting phases, and the high CaO ratio, the clay of the region started to sinter after firing and the transition to phase transformations began.

In addition, in Fig.8 when the XRD phases of the raw clay and fired clay samples are examined, it can be said that the clays contain muscovite/illite phase, quartz, and a small amount of calcite phase. After firing, it was observed that the crystallinity of the clay minerals phases increased, and more severe quartz phases emerged.

Figure. 8. XRD results of raw clay and fired clay samples / *Ham kil ve pişmiş kil örneklerinin XRD sonuçları.*

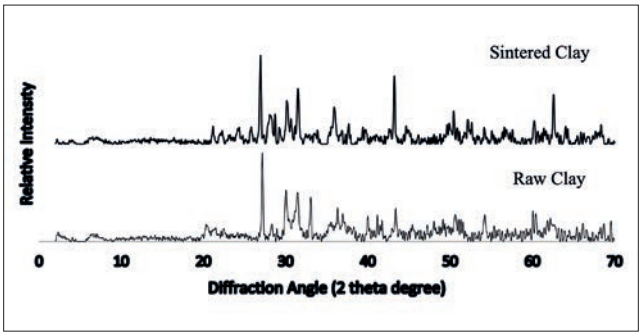

Figures 9 show the XRD analysis phases of the finds belonging to the EBA-III period. By comparing the relative intensities of the phases formed in the qualitative analysis results, the stages determined according to the PDF cards of the JADE analysis program can be interpreted.

In the samples, it is seen that the dominant phases are mostly quartz (PDF=98-020-0727), anorthite (PDF=98-020-1644, and a small amount of muscovite (PDF-98-006-8548), illite (PDF=98-009-0144) phase.

In the comparative XRD phase analysis table in Figure 9, where the samples from the EBA-III period were exposed to fire at different rates, the amorphous and crystalline states of the samples, the relative increases, and decreases in the phases are seen. When the XRD analysis of the EBA-III-7 graph, which is thought to be exposed to the most oxidation conditions, is examined, it is believed that the crystallization is high, and the clay used in the mud brick is exposed to heat. The change in intensity of the quartz phase, the formation, and quantitative differences in the anorthite phase, and the presence and evolution of the muscovite degree in XRD are seen. The change in the state of being exposed to fire is from most to low; the samples exposed to the highest fire are EBA-III-7, EBA-III-6, EBA-III-5, EBA-III-4, EBA-III-3, EBA-III-2, EBA-III-1 respectively.

Figure 9. XRD results of EBA-III mud brick samples. (Q: Quartz, A: Anorthite, M: Muscovite)/ EBA III kerpiç buluntularının XRD sonuçları. (Q: Kuvars, A: Anortit, M: Muskovit).

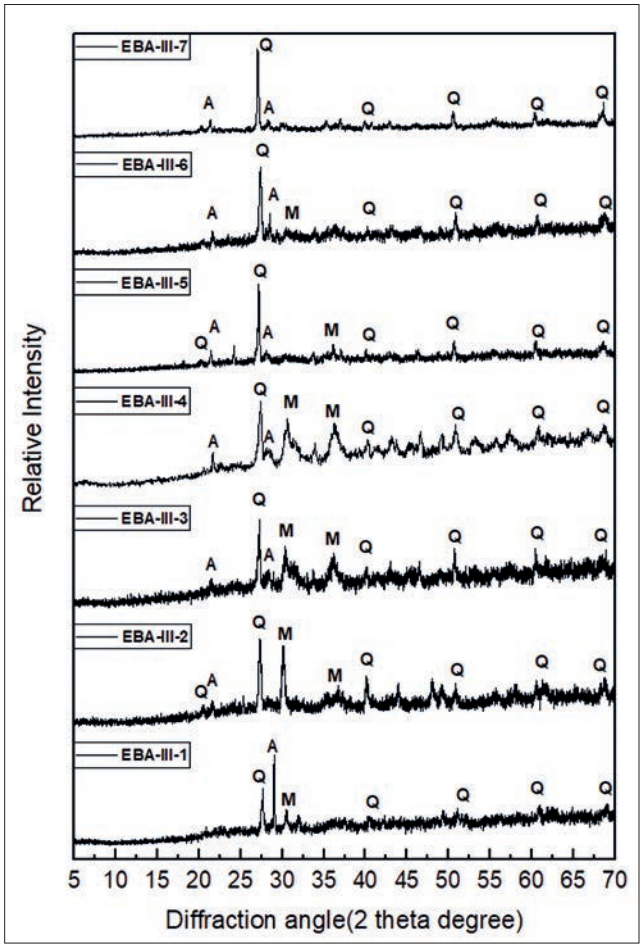

Figure 10 shows the XRD analysis phases of the findings belonging to the MBA period. By comparing the relative intensities of the phases formed in the qualitative analysis results we have examined here, the stages determined according to the PDF cards of the JADE analysis program can be interpreted. When the Middle Bronze Age samples are analyzed, it is seen that the examples contain quartz (PDF=98-020-0727), anorthite (PDF=98-020-1644), a small amount of muscovite (PDF-98-006-8548), illite (PDF=98-009-0144) and a small amount of calcite. In XRD data, it can be said that MBA-1 and MBA-2 are less fire, and MBA-3 was exposed to a higher temperature. It can be said that MBA-1 is exposed to more fire than MBA-2 (it can be evaluated by analyzing the intensity of muscovite and quartz peaks, which are approximately 30 degrees in MBA-2).

Figure 10. XRD results of MBA mud brick samples. (Q: Quartz, A: Anorthite, M: Muscovite)/MBA kerpiç buluntularının XRD sonuçları. (Q: Kuvars, A: Anortit, M: Muskovit).

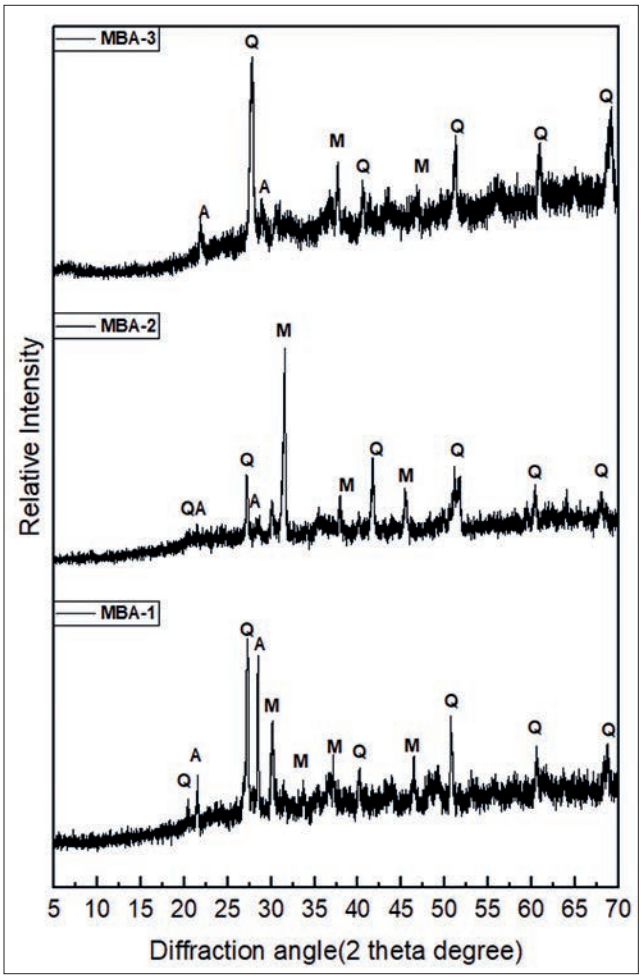

Figure 11, Figure 12, and Figure 13 show the FTIR graphs of samples from clay-fired clay, EBA-III period, and MBA period, respectively. It is seen that the results are complementary to XRF, and XRD analyses. In some previous studies, it was seen that FTIR was used to examine the effects of carbonaceous particles exposed to SO_2 on different building materials.

DOI: 10.22520/tubaar.1374064

Figure 11. FTIR results of clay and fired clay samples / *Ham kil ve Pişmiş kil numunelerinin FTIR sonuçları.*

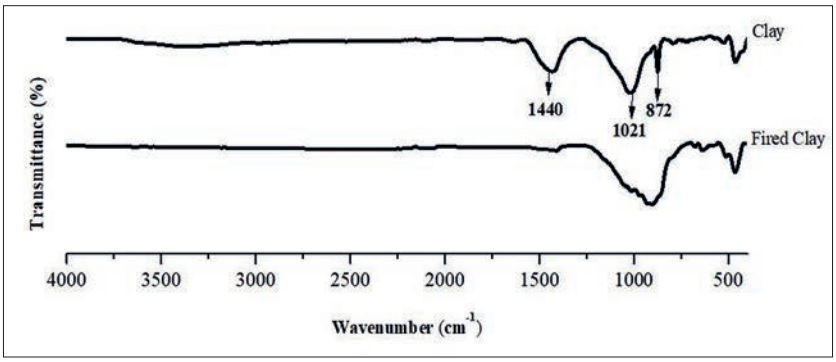

Figure 12. FTIR results of EBA-III mud brick samples / *EBA III kerpiç buluntularının FTIR sonuçları.*

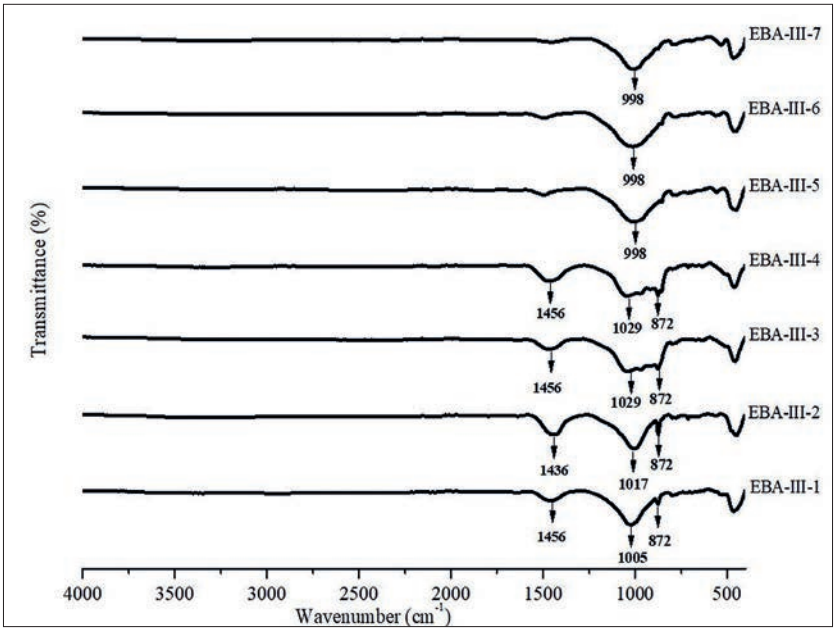

Figure 13. FTIR results of MBA mud brick samples / *MBA kerpiç buluntularının FTIR sonuçları.*

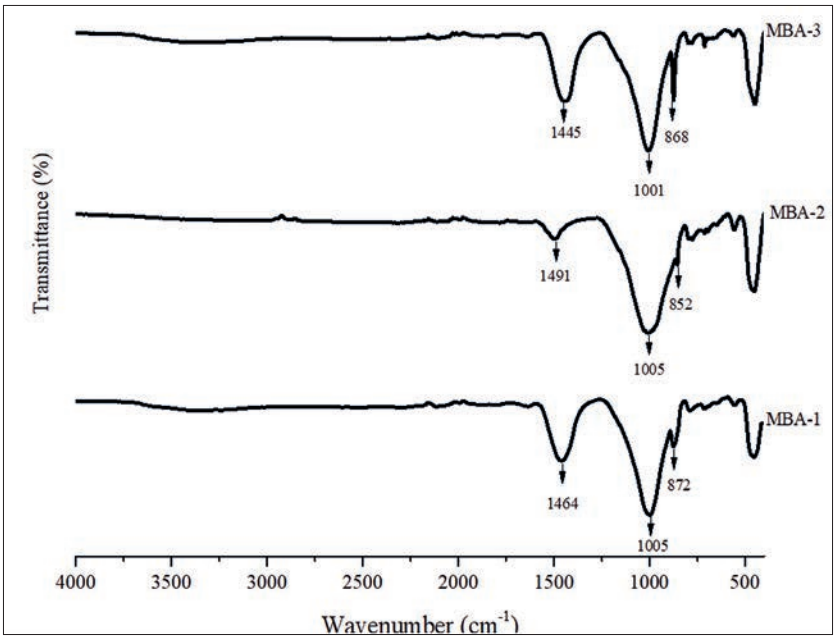

When the FTIR analyses of the finds and clay samples are examined, the peaks seen around 500 cm^{-1} belong to the silicon atom with a coordination number of four with oxygen (Khale and Chaudhary 2007, Yunsheng, et al, 2007). These peaks are from quartz crystals.

In aluminosilicate materials containing clay, such as clay and adobe, Si-O-Si or Al-O-Si asymmetric stretching peaks occur at 990 - 1090 cm^{-1}. FTIR analysis of calcined clay or mud bricks presumably exposed to fire, shows that this peak has shifted to around 989 cm^{-1}. It is thought that the decrease of this value to lower values is due to the partial replacement of SiO_4 tetrahedrons by AlO_4 tetrahedrons. This situation represents the change in structure due to exposure to fire (Ormancı et al. 2024, Khale and Chaudhary 2007, Panias et al. 2007, Perisic et al. 2016).

The stretching vibrations of $CaCO_3$ with peaks at 1440-1500 cm^{-1} and 850-872 cm^{-1} have been identified in samples (Melo, et al. 2014; Ormancı, et al. 2024).

In the FTIR spectra of calcined clay and fire-exposed EBA III 5-6-7 samples in Figures 11 and 12, the peaks around 1450 and 870 cm^{-1} are significantly reduced and disappeared. This indicates that carbonates leave the structure with exposure fire.

Fire ignites organic-based additives in building materials such as mud brick and plaster causing various types of damage to the material. If the temperature rises above 200 degrees at the start of the fire, the bound water in the mud brick and application begins to move away from the body. When the temperature rises above 450-600 °C, the organics, organic matter is removed and colour changes occur (Duran et al. 2016). Depending on the amount of oxygen during the fire, the mud bricks turn into light brown, orange, and red. Depending on the type and mineralogical properties of the clay used during production, the clays begin to solidify structurally and retain their porous structure. When the temperature reaches 950°C, the porosity of the alumina silica structures decreases, and the vitrification process begins. At higher temperatures (1000-1400 °C), tridymite and cristobalite is observed (Uz and İssi 2015).

With the XRF, XRD, and FTIR analyses performed in the study, a comparison could be made on the fire exposure rates of the EBA-III and MBA period samples. The interpretations made on fire sightings with the pieces selected from the samples of this period gain integrity with SEM-EDX analyses.

Figure 14. SEM analysis of EBA-III mud brick samples / *EBA III kerpiç buluntularının SEM analizi.*

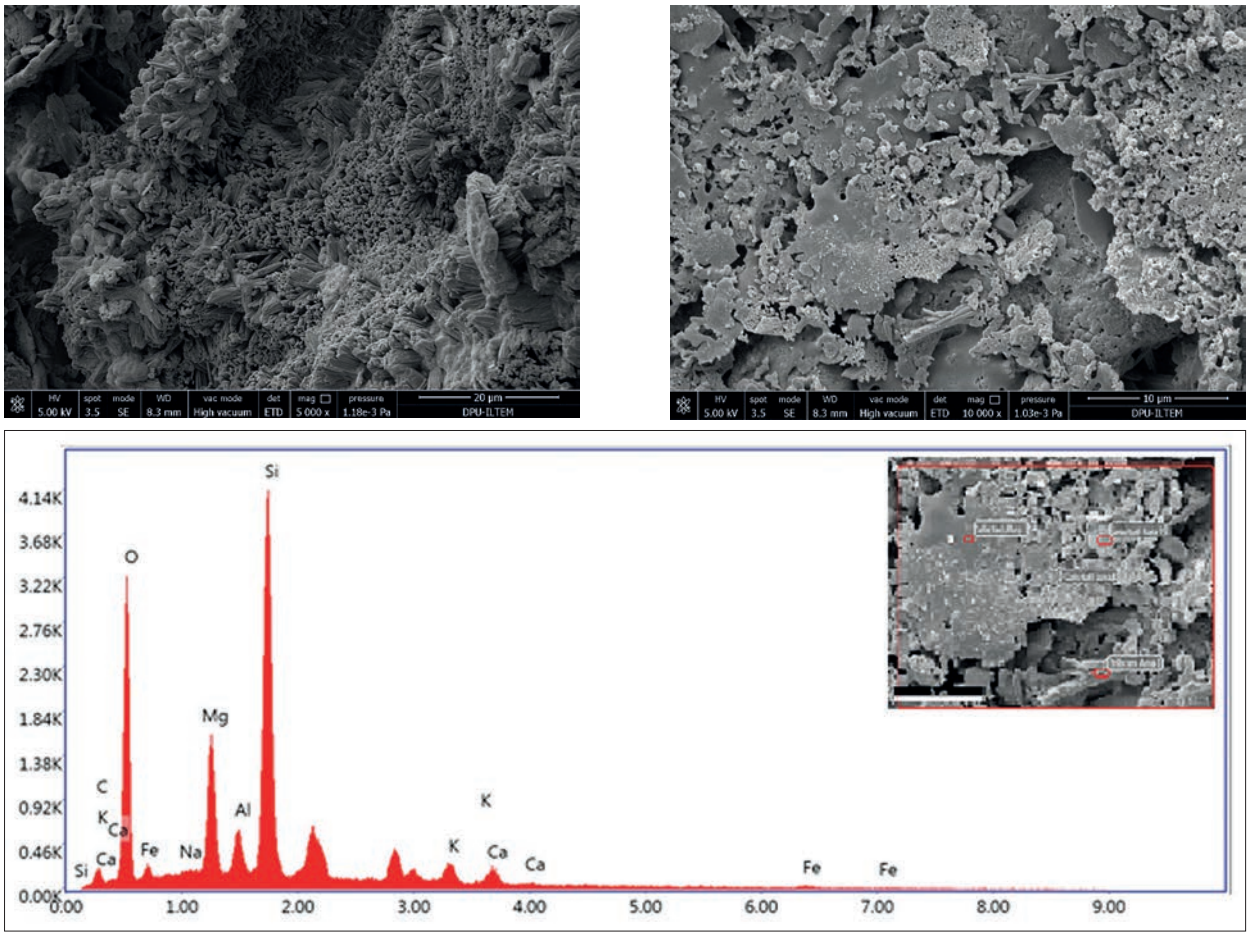

DOI: 10.22520/tubaar.1374064

It is seen that the EBA III-2 sample selected in Figure 14 is more exposed to fire than the other samples. Looking at the SEM images of the sample, it is seen that there is vitrification in the structure and the grains merge in places and form the beginning of sintering. This situation shows us that the sample was exposed to high temperature and the materials reacted with the effect of heat and formed a glass structure. According to the EDX analysis point analysis results of the EBA-III-2 sample in Table 3, it is seen that there is a high proportion of Al_2O_3, SiO_2, and a low proportion of CO_3.

Table 3. SEM-EDX analysis results of the mud brick sample no. EBA-III-2 / *EBA III-2 nolu kerpiç buluntusuna ait EDX analiz sonuçları.*

Element	1.Weight %	2.Weight %	3.Weight %	4.Weight %
CO_3	0.02	0.02	0.01	0.03
CaO	8.7	15.2	10.3	8.1
Fe_2O_3	2.0	3.3	0.05	0.7
Na_2O	1.1	0.8	0.8	0.9
MgO	15.4	7.8	5.8	4.4
Al_2O_3	7.6	11.4	18.0	21.8
SiO_2	65.2	61.7	65.0	63.9

Figure 15 shows the SEM analysis of the EBA III-5 sample. Here, it can be seen from the structural XRD and the chemical analysis results in XRF that the sample is exposed to fire at a lower rate. SEM analysis also supports these results. In the SEM images of the EBA III-5 sample, it was observed that the layered clay structure was preserved, while the scaly structure of the clays was observed. This indicates that the clay structure has not deteriorated, and the firing temperature of this type of sample is not exposed to heat up to the decomposition temperature of the clay. The presence can make this interpretation of clay structures here. According to the EDX analysis point analysis results of the EBA III-5 sample in Table 4, a high rate of K_2O and CO_2 presence is seen in the point analyses taken from three points. It was observed that the amounts of SiO_2 and Al_2O_3 were lower than the EBA III-2 sample. In other words, the vitrification rate of the clay-like structure is relatively low compared to the other group of the same period. Therefore, it can be said that the fire exposure rate of this sample is less.

Figure 15. SEM analysis of the EBA-III-5 mud brick samples / *EBA III-5 kerpiç buluntularının SEM analizi.*

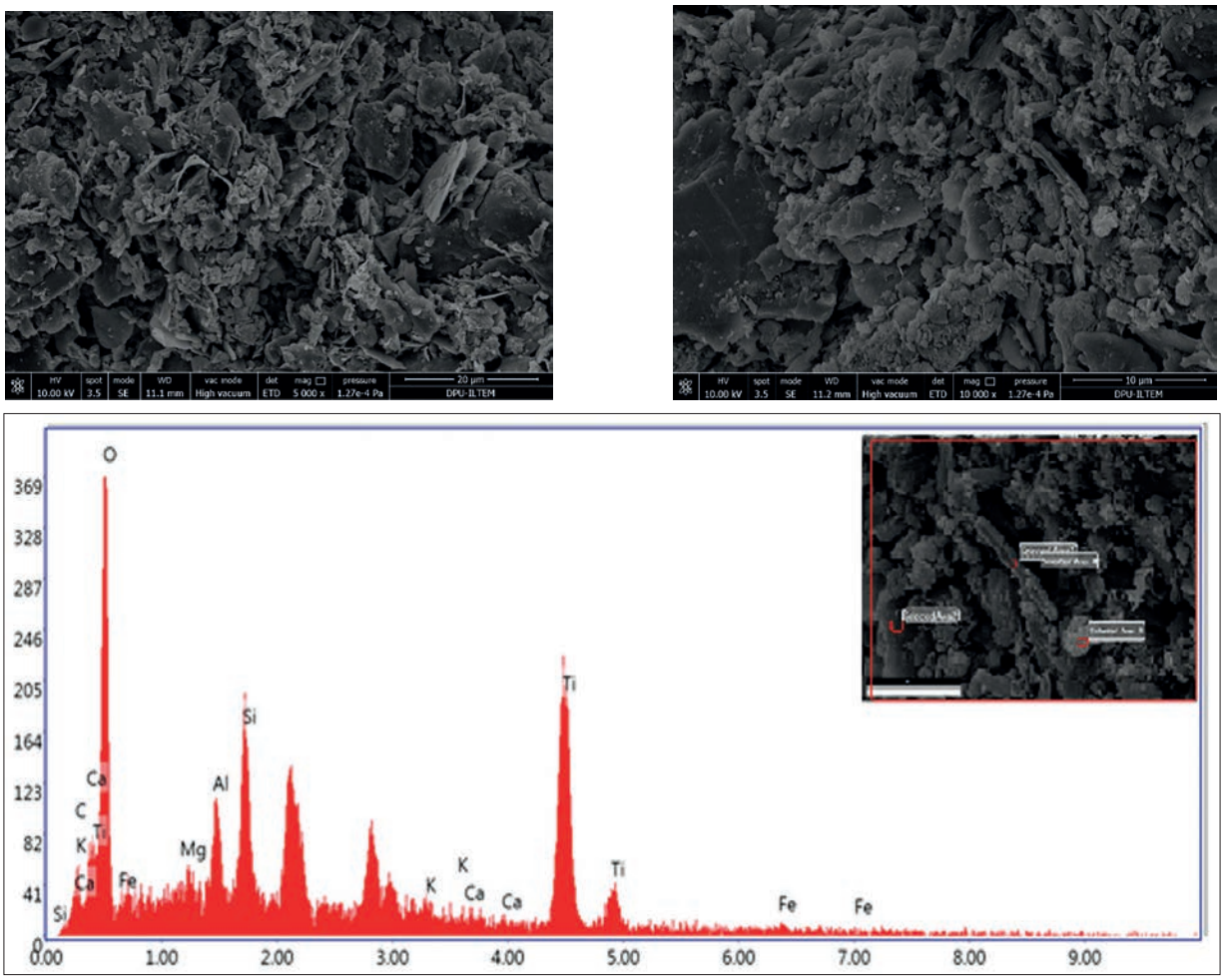

Table 4. SEM-EDX analysis results of the mud brick sample no. EBA-III-5 / *EBA III-5 nolu kerpiç buluntusuna ait EDX analiz sonuçları.*

Element	1.Weight %	2.Weight %	3.Weight %	4.Weight %
K_2O	8.1	48.9	6.3	6.5
CO_3	8.4	11.9	13.6	13.1
CaO	9.7	6.4	7.4	8.1
Fe_2O_3	1.5	1.4	1.7	1.6
MgO	6.4	1.03	4.6	4.8
Al_2O_3	16.5	4.8	14.9	17.5
SiO_2	49.1	17.2	51.2	48.2

Figure 16 shows the SEM image of the MBA-2 sample. In XRF, XRD, and FTIR analyses of this sample, it was demonstrated that it was less exposed to fire or did not see fire. Clay structures and some rod-like organic structures are seen in the images with the SEM analysis results. These images show that the mudbrick sample's clay and organics were not exposed to fire. In addition, according to the EDX point analysis results given in Table 5, a high percentage of CO_3 and a lower percentage of SiO_2 and Al_2O_3 oxides are seen.

Table 5. SEM-EDX analysis results of the mud brick sample MBA-2 / *MBA-2 nolu kerpiç buluntusuna ait EDX analiz sonuçları.*

Element	1.Weight %	2.Weight %
CO_3	25.1	22.8
CaO	24.5	17.4
Fe_2O_3	0.4	0.8
MgO	4.6	6.1
Al_2O_3	9.7	12.5
SiO_2	35.6	40.1

Figure 17 shows the SEM image of the MBA-3 sample. This sample was said to have seen fire in XRF, XRD, and FTIR analysis. With the SEM analysis results, the glassy structure is seen intensely in the structure. Therefore, it is an indicator that the samples are exposed to high temperatures. This shows that the mud-brick samples may have seen and suffered a fire. When the EDX point analysis results of the MBA-3 model are examined in Table 6, it is seen that there is a shallow rate of CO_3 and a high rate of SiO_2 and Al_2O_3 in the structure. When these oxides are higher than MBA-2, and combined with other analysis results, we can say that this sample was less exposed to fire than the find, which is thought to be from the same period.

Figure 16. SEM analysis of MBA-2 mudbrick samples / *MBA-2 kerpiç buluntularının SEM analizi.*

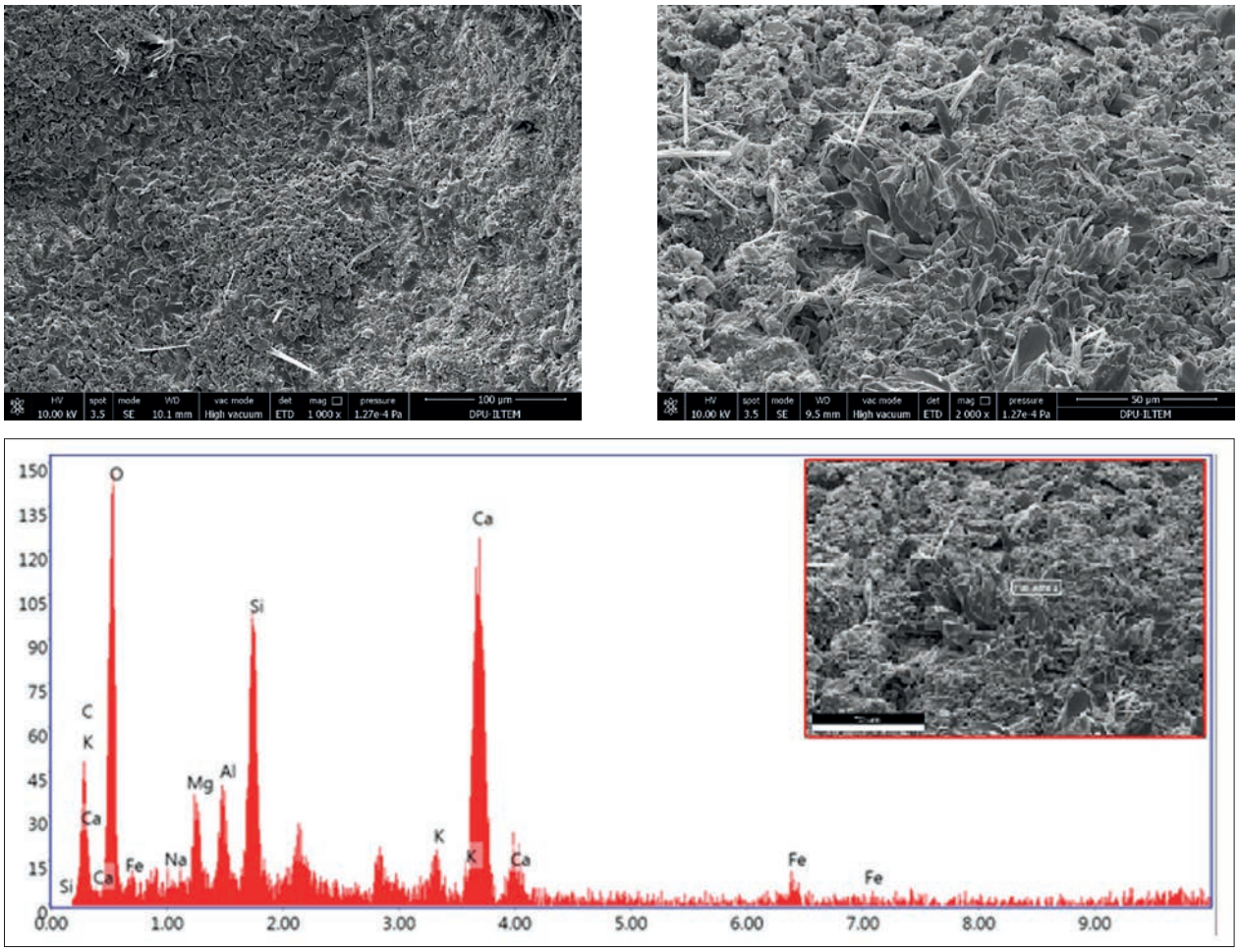

DOI: 10.22520/tubaar.1374064

Fig. 17. SEM analysis of MBA-3 mud brick samples / *MBA-3 kerpiç buluntularının SEM analizi.*

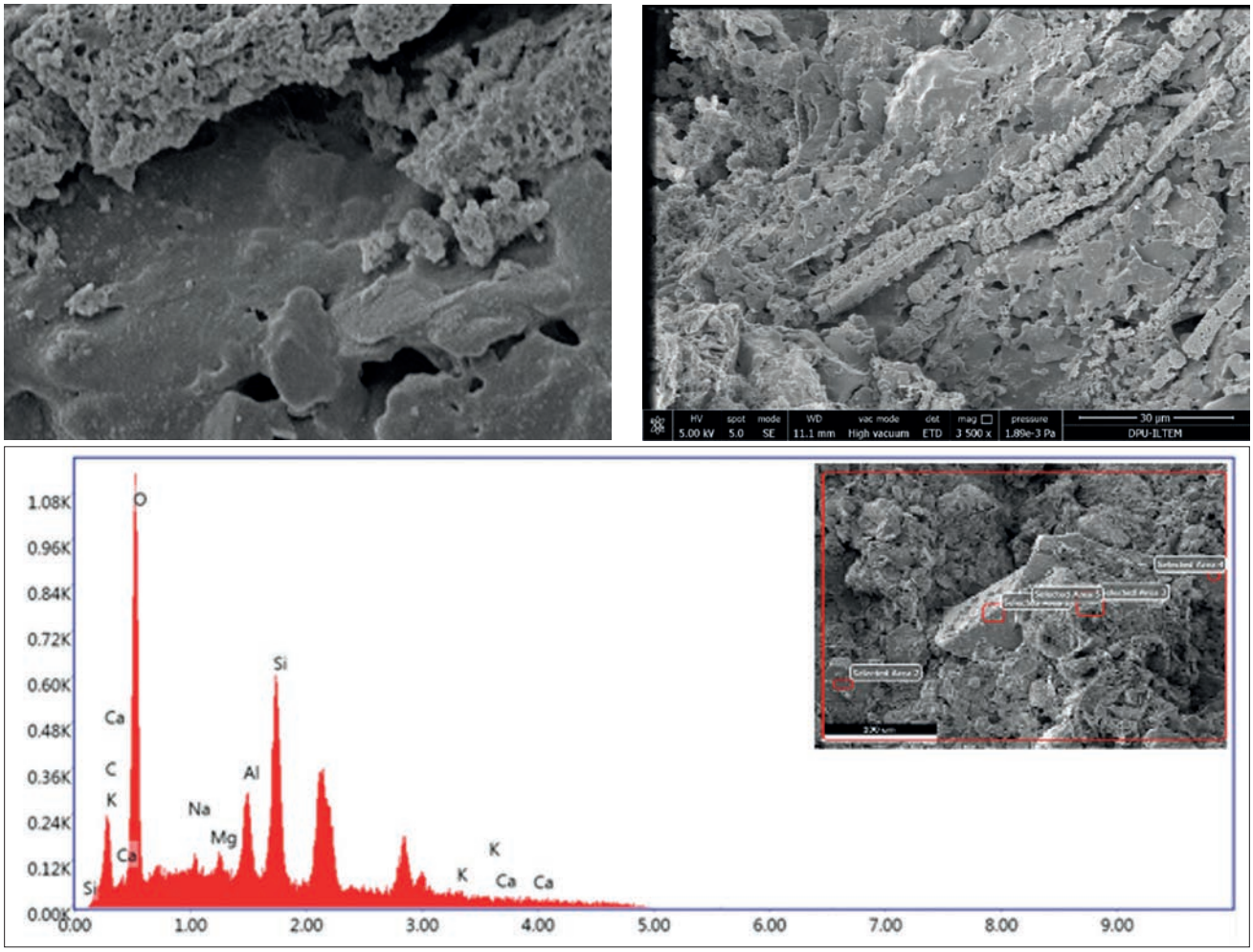

Table 6. SEM-EDX analysis results of the mud brick sample MBA-3 / *MBA -3 nolu kerpiç buluntusuna ait EDX analiz sonuçları.*

Element	1.Weight %	2.Weight %	3.Weight %	4.Weight %
CO_3	0.02	0.02	0.02	4.4
CaO	12.7	11.0	12.7	10.2
Na_2O	2.3	1.4	2.3	2.8
MgO	5.7	6.7	5.7	8.5
Al_2O_3	20.2	21.8	20.2	23.5
SiO_2	59.0	58.9	59.0	50.4

CONCLUSIONS

The 12 mudbrick finds belonging to the EBA-III period and V/D phase of the MBA period, which were recovered from the Seyitömer Höyük region in 2021, were classified chronologically in chronological order.

In addition, the samples of the clay obtained from the region were also made and compared with those of the EBA-III and MBA mud-brick samples. According to the analysis results, the quartz, anorthite, and muscovite ratios contained in the regional clay support the view that the nearby clay deposits were used to construct the settlements.

It is observed that in both periods (EBA III and MBA), similar methods (such as using a regional clays and kaolins formed for these mud bricks) were used to form adobe mortar, and no different materials were added. Therefore, it is possible to say that the settlers maintained a certain tradition in mudbrick making.

EBA III and MBA periods are chronologically consecutive periods. These two periods constitute a historical period of approximately 750 years. As a result of the archaeological excavations, it was determined that the mudbrick finds representing different periods were produced with similar raw materials and methods.

In addition, the differences in the mudbrick structures between the periods shown in the characterisation studies are thought to be the result of periodic earthquakes, fires and various natural events.

It is possible to say that the mudbrick sampled spaces were exposed to fire to a greater or lesser extent except for MBA (IV/C). Since the XRF analyses of EBA-III (V/B), EBA-III (V/C), EBA-III (V/C), EBA-II-III (VI), and MBA-IV samples showed high fire loss and SEM image analyses showed glazing in these mudbrick samples, it can be said that the fire in the sampled spaces reached up to 900℃. In the places where EBA-III V/D, EBA-III V/D, EBA-III (V/D), and MBA-(IV/C) samples were taken, it is understood that the fire reached 450-600℃.

The four-phase EBA III period, which covers a total period of 750 years at Seyitömer mound, and the subsequent MBA period are valuable in terms of further defining the mudbrick building materials and defining the conditions to which the surviving structures were exposed. The information obtained can guide the identification of mudbrick building materials from the EBA III and MBA periods and archaeometric studies.

Acknowledgments

The authors thank Mr. Serdar Unan, who is responsible for the Seyitömer Höyük Rescue Excavation for the period 2019-2021, for their support in providing the samples in this study, as well as Mehmet Akkas, M.Sc Engineer from İLTEM research center who carried out the analysis, and DPU BAP 2021-03 for their support for the project.

REFERENCES

Akkas, F., 2011. Investigating the Production Possibilities of Fibre-Reinforced Mud Brick Panel Wall. Istanbul Technical University, Institute of Science, Master's Thesis, İstanbul.

Bilgen, A. N., 2012. Seyitomer Hoyuk 2011 Excavation Report. Kutahya.

Bilgen, A. N., Bilgen, Z., 2015. Middle Bronze Age Settlement (IV. Layer). *Seyitomer Hoyuk I*, Pp. 61-118, İstanbul.

Bilgen, A. N., Bilgen, Z., Cırakoglu, S., 2015. Early Bronze Age Settlement (V. Layer). *Seyitomer Hoyuk I*, Pp. 119-186, İstanbul.

Dirican, T., Akyol, A. A., 2019. A Compilation Study of Mud Brick Wall Construction Methods in Anatolia. *Sanat ve Tasarım Dergisi*, (23), Pp. 117-126.

Duran S., Cakırozu Civelek F., Aktuglu Y.K., 2016. Roof and Facade Materials in Adobe Buildings; Aksehir, Erdogdu, and Menderes Examples. *8. National Roof & Facade Symposium*, 2– 3 June 2016 Mimar Sinan University of Fine Arts, İstanbul.

İlaslı, A., 1996. Seyitomer Hoyugu 1993 Rescue Excavations, *6. Mkks*, 24- 26 Nisan 1995 Didim, Ankara, S. 1-15.

Khale, D., Chaudhary, R., 2007. Mechanism of Geopolymerization and Factors Influencing ıts Development: A Review, J Mater Sci, 42:729–746

Melo, H. P., Cruz, A. J., Candeias, A., Mirão, J., Cardoso, A. M., Oliveira, M. J., & Valadas, S., 2014. Problems of Analysis by FTIR of Calcium Sulphate–Based Preparatory Layers: The Case of a Group of 16th-Century Portuguese Paintings. Archaeometry, 56(3), 513-526.

Ormancı, Ö. Atasayar, Z., & Boso Hanyalı, Ö. 2024. Investigating the Middle Iron Age ceramics of Van Fortress through multi-analytical techniques. Spectrochimica acta. Part A, Molecular and biomolecular spectroscopy, 313, 124103.

Ozcan, N., 1986. Seyitomer (Kutahya) Palynological Properties of Lignites. Dokuz Eylül University Graduate School of Natural and Applied Sciences, Master's Thesis, İzmir.

Ozdogan, M. 1996. From Cottage to Housing: Firsts in Architecture. *Housing and Settlement in Anatolia from History to Present*. Pp. 19-30, İstanbul.

Panias, D., Giannopoulou, I. P., Perraki, T., 2007. Effect of synthesis parameters on the mechanical properties of fly ash-based geopolymers, Colloids and Surfaces A: Physicochem. Eng. Aspects 301:246–254

Perisic, N.; Maric-Stojanovic, M.; Andric, V.; Mioc, U., 2016. Damjanovic, L. Physicochemical Characterisation of Pottery from the Vinca Culture, Serbia, Regarding the Firing Temperature and Decoration Techniques. J. Serbian Chem. Soc. 81, 1415–1426

Qiu, G., Li, G., Fan, X., Huang, Z.,2004. Activation and removal of silicon in kaolinite by thermochemical process. Scandinavian Journal of Metallurgy, SCAND J METALL. 33. 121-128.

Topbas, A., 1992. Kutahya Seyitomer Hoyugu Rescue Excavation 1990. *Iı. Mkks*, 29- 30 April 1991 Ankara, Ankara, Pp. 11-27.

Topbas, A., 1993. Seyitomer Hoyugu Salvage Excavation in 1991. *Iıı. Mkks*, 27- 30 April 1992 Efes, Ankara, Pp. 1-30.

Topbas, A., 1994. Seyitomer Hoyugu 1992 Salvage Excavation. *Iv. Mkks*, 26- 29 April 1993 Marmaris, Ankara, Pp. 297-301.

Unan, N., 2013. Material and Technical Evaluation of Seyitomer Architecture. *Kubaba 22,* Pp. 7-19.

Unan, N., 2019. Seyitomer Hoyuk Investigation of Grain Production and Storage Activities in the Middle Bronze Age. *Kutahya Arkeoloji, Sanat Tarihi Ve Tarih Arastırmaları,* Ankara, Pp. 111-126.

Unan, S., Unan, N., Bilgic, H., Andac, M., 2020. Seyitomer Hoyuk Rescue Excavation 2019. *Kutahya Arkeoloji, Sanat Tarihi Ve Tarih Arastırmaları*, Ankara, Pp. 1-16.

Unan, S., Unan, N., Bilgic, H., Andac, M., 2021. Seyitomer Hoyuk Rescue Excavation Works for 2020, *Kutahya Arkeoloji, Sanat Tarihi Ve Tarih Arastırmaları*, Ankara, Pp. 1-19.

Uz, V., Deniz, S., İssi, A., Bilgen, A. N. 2015. Investigation of the Roman period pottery production technology from the Seyitömer Mound (Kutahya/Türkiye). *WIT Transactions on The Built Environment*, 168, 627-635.

Yanık, G., 1997. Geology, Mineralogy and Uses in Ceramic Industry of Seyitomer (Kutahya) Comur Basin Clays. Dumlupınar University Graduate School of Natural and Applied Sciences Master's Thesis, Kutahya.

Yunsheng, Z., Wei, S., Zongjin, L., 2007. Preparation and microstructure of K-PSDS geopolymeric binder, Colloids and Surfaces A: Physicochem. Eng. Aspects, 302:473–482.

Yuzbasıoglu, N., 2010. The Development and Characteristics of Seyitomer Civil Architecture. Dumlupınar University, Institute of Social Sciences, Department of Archeology, Unpublished Master's Thesis, Kutahya.